International Journal of Heat and Mass Transfer 145 (2019) 118698

Contents lists available at ScienceDirect

International Journal of Heat and Mass Transfer

journal homepage: www.elsevier.com/locate/ijhmt

Theoretical modeling and optimization of fin-based enhancement of heat transfer into a phase change material

Amirhossein Mostafavi, Mohammad Parhizi, Ankur Jain *

Mechanical and Aerospace Engineering Department, University of Texas at Arlington, Arlington, TX, USA

ARTICLE INFO

Article history:
Received 23 January 2019
Received in revised form 1 May 2019
Accepted 4 September 2019

Keywords:
Phase change materials
Energy storage
Extended surfaces
Theoretical modeling

ABSTRACT

Phase change heat transfer is used commonly for enhanced thermal management and energy storage in several engineering applications. The rate of heat transfer from a heat source into a phase change material (PCM) is limited by thermal properties and geometry, due to which, the use of metal fins protruding into the PCM has been investigated. This paper derives and solves the governing energy conservation equations to determine the transient temperature distribution in the PCM due to the presence of a Cartesian fin. A perturbation method based solution for the Stefan problem with time-dependent temperature boundary condition is used to derive an equation for the fin temperature distribution. Results show that for a given total time available for heat transfer into the fin, the presence of a fin results in two competing effects – enhanced heat transfer into the PCM through the fin and reduced heat transfer into the PCM due to lower area of direct contact between PCM and heat source. This results in a non-monotonic dependence of total heat flow into the PCM on the fin size, and shows that a fin larger than a certain optimal size may actually impede overall heat flow into the PCM. For a given total time, the optimal fin size is shown to be a function of the fin thermal conductivity. The impact of thermal properties of PCM and fin on the rate of heat transfer is also examined. The theoretical work in this paper extends the well-known governing equation for a fin in a single-phase medium to a fin in a phase change material, which is a much more complicated, transient problem. In addition to extending the theoretical understanding of extended surfaces and phase change, this work also provides practical guidelines for the optimized design of phase change based energy storage and thermal management systems.

1. Introduction

Phase change based energy storage plays a key role in several engineering applications [1–3]. Due to the significantly large latent heat compared to specific heat capacity, phase change offers much greater energy storage capability compared to sensible heat based technologies [4]. A key challenge in phase change energy storage, however, is that thermal impedance offered by the melted phase results in a reduction in the rate of heat transfer to the phase change propagation front.

Due to this self-limiting nature of the phase change propagation process, several approaches for enhancement in phase change based energy storage have been investigated, including the insertion of fins into the PCM [5–7]. Fins offer potential improvement in rate of energy stored by enhancing available surface area for heat transfer into the PCM. A key goal of research in this field has been to optimize fin shape and size for enhanced rate of energy storage. Towards this, both experimental and theoretical/numerical research has been reported.

On the experiments side, two-dimensional melting in a PCM with convection in the liquid has been experimentally investigated in both vertical and horizontal configurations of a finned tube storage unit [8,9]. Melt fraction has been shown to be a function of both Stefan and Fourier numbers, with conduction being the dominant heat transfer mode at the beginning of melting [8,10]. Presence of a fin has been shown to result in improved performance of a PCM-based heat sink [11]. Melting fraction and fin effectiveness have been experimentally correlated for horizontal fins in a rectangular enclosure [12]. Dimensionless correlations for fin effectiveness in melting and solidification processes have been developed [13]. The impact of geometry on the importance of convective effects has been investigated [14]. Comparison of experimental data and numerical model prediction for different configurations of a photovoltaic-PCM system with internal fins has been presented [15].

Significant research on theoretical and numerical modeling of fin-based heat transfer into a PCM is also available. The PCM

* Corresponding author at: 500 W First St, Rm 211, Arlington, TX 76019, USA.
E-mail address: jaina@uta.edu (A. Jain).

https://doi.org/10.1016/j.ijheatmasstransfer.2019.118698
0017-9310/

Nomenclature

c	volumetric heat capacity (J/m^3 K)
C_p	specific heat capacity (J/kg K)
$\overline{c}_f$	non-dimensional fin volumetric heat capacity, $\overline{c}_f = \frac{c_f}{c_p}$
k	thermal conductivity (W/m K)
$\overline{k}_f$	non-dimensional fin thermal conductivity, $\overline{k}_f = \frac{k_f}{k_p}$
L	fin length (m)
$\overline{L}$	non-dimensional fin length, $\overline{L} = \frac{L}{W}$
L_p	latent heat of fusion (J/kg)
q	heat absorbed per unit depth (J/m)
$\overline{q}$	non-dimensional heat absorbed, $\overline{q} = \frac{q}{(T_w - T_m)c_p W^2}$
q''_{f-p}	heat flux from fin into PCM (W/m^2)
Q''	thermal conduction heat flux (W/m^2)
$\overline{S}$	non-dimensional source term, $\overline{S} = \frac{q''_{f-p} W}{\frac{w}{W}(T_w - T_m)k_f}$
Ste	Stefan number, $Ste = \frac{C_p(T_w - T_m)}{L_p}$
t	time (s)
$\overline{t}$	non-dimensional time, $\overline{t} = \frac{\alpha_p t}{W^2}$
T	temperature (K)
T_m	phase change temperature (K)
T_w	wall temperature (K)
w	fin width (m)
W	width of the domain (m)
x,y	spatial coordinates (m)
$\overline{x}, \overline{y}$	non-dimensional spatial coordinates, $\overline{x} = \frac{x}{W}$, $\overline{y} = \frac{y}{W}$
x_{LS}	location of phase change front originating from fin (m)
$\overline{x}_{LS}$	non-dimensional location of phase change front originating from fin, $\overline{x}_{LS} = \frac{x_{LS}}{W}$
y_{LS}	location of phase change front originating from fin (m)
$\overline{y}_{LS}$	non-dimensional location of phase change front originating from fin, $\overline{y}_{LS} = \frac{y_{LS}}{W}$

Greek symbols

α	thermal diffusivity (m^2/s)
β	non-dimensional eigenvalues
θ	non-dimensional temperature, $\theta = \frac{T - T_m}{T_W - T_m}$
λ	non-dimensional eigenvalues

Subscripts and superscripts

f	fin
p	phase change material
*	initial approximation

melting process within vertical fins attached to a horizontal constant temperature plate has been studied numerically to study the effect of fin geometrical parameters on the melting process. Dimensional analysis has been carried out to generalize the results for determining melt fraction [7]. Semi-analytical and numerical modelings of melting and solidification processes in the presence of a fin have been presented [16–18]. The fraction of solidified PCM and fin temperature distribution in a PCM heat sink with plate fins has been calculated using a simplified analytical model for constant heat flux boundary condition [19]. Numerical methods have been used to optimize fin geometry for maximizing phase change based heat sink performance [20], to determine the critical size of a composite heat sink [21] and to minimize the length of a finned storage system to meet the criteria for the critical operation time in electronic devices [22]. Experimental and numerical investigation of a PCM based heat sink with straight fins has been presented [23]. This work showed that fin geometry affects heat sink performance, and an optimal fin thickness results in maximum rate of heat removal [23]. Numerical optimization of the number and size of fins with constant heat flux boundary condition has also been presented [24]. Solidification time has been approximated using an approximate analytical method for two different finned storage systems [25]. An analytical solution has been compared with a numerical method to estimate the solid-liquid interface in a finned PCM storage system [19].

Fig. 1 shows a schematic of a simplified Cartesian phase change based energy storage, wherein the PCM absorbs heat from two hot walls maintained at a constant temperature. A fin protruding between the walls into the PCM results in enhanced available surface area for heat transfer into the fin. Note that if infinite time is available for heat transfer from the wall into the PCM, then the entire PCM will melt and reach the wall temperature. In such a case, the total amount of energy that can be stored is known in advance, and the presence of the fin is actually counterproductive, since it reduces PCM volume. However, in many practical applications, only a finite amount of time is available for effecting the heat transfer process, in which case, the presence of the fin may be beneficial, depending on the balance between two key heat transfer effects. On one hand, the presence of a fin reduces PCM volume available and the area of direct contact between the PCM and the hot wall. In Fig. 1, for example, the fin of width *2w* results in only the remainder *2(W-w)* width of the hot wall being available for direct heat transfer into the PCM. This results in reduced heat transfer from the wall to the PCM. On the other hand, however, thermal conduction occurs from the hot wall into the fin, followed by heat transfer from the fin surface into the PCM. This is a transient process, because of the time involved in thermal diffusion into the fin. Initially, the fin temperature is not very high, due to which, it does not enhance heat transfer into the PCM. As time passes and the fin heats up, it increasingly contributes towards heat transfer into the PCM. Due to these two directly conflicting effects of the fin and the transient nature of this problem, it is possible that for a given, finite time available, an optimal fin size may exist that results in enhanced energy storage despite the reduced PCM volume due to inclusion of the fin. A theoretical heat transfer model for this problem is very desirable for studying such transient effects. Some work in this direction has been reported by Lamberg & Sirén, who presented semi-analytical and numerical solutions for melting and solidification processes in the presence of a fin [16–18]. Through simplifying assumptions of quasi-steady conditions and no sensible heat storage, governing equations for the fin temperature and phase change front location were derived. An expression for the fin temperature was obtained by assuming the phase change front location to be constant. While this approach resulted in a solution for the fin temperature, some of these assumptions may not be accurate, and it may be helpful to account for effects neglected in these papers. Further, these papers do not address the conflicting effects of the fin on energy absorbed in the PCM as outlined above, and the consequent optimization problem of maximizing heat transfer into the PCM for a given total time as a function of fin size and thermal properties. A comprehensive theoretical heat transfer model is needed to optimize the use of fins for enhancing heat transfer in PCMs and exploring optimal fin size.

This paper derives the governing energy equation for heat transfer from a hot wall into a PCM in the presence of fins extending into the PCM. The equation accounts for transient thermal diffusion into the fin and the resulting transient heat transfer into the PCM. Both latent and sensible heat storage in the fin are accounted for. Based on a semi-analytical solution of the equation, an expression for the total heat absorbed by the PCM for a given total time is

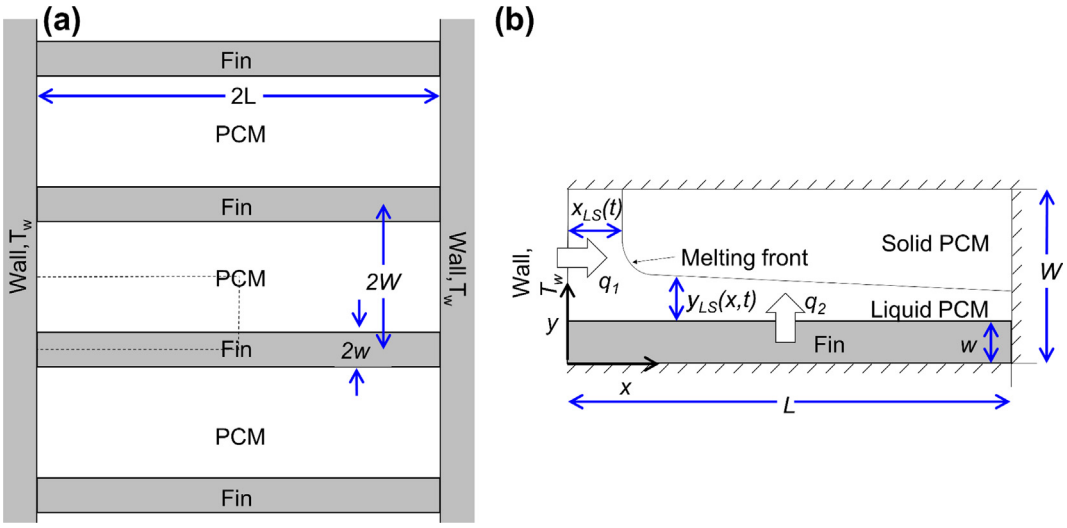

Fig. 1. (a) Schematic of a Cartesian phase change energy storage problem with periodic fins for enhancing energy storage in the PCM; (b) Schematic of the unit cell in this heat transfer problem.

derived. This is used to examine the dependence of total heat absorbed on the fin size, showing that, for a given total time, the total heat absorbed is highest at a specific fin size. This optimal fin size is itself shown to be a function of fin thermal conductivity, as well as the total time available. These results provide useful insights into the nature of enhanced heat absorption into a PCM due to a fin, and help in optimizing the fin design in order to maximize heat absorption into the PCM.

2. Theoretical model

Consider a wall maintained at a constant temperature T_w, from which, thermal energy is absorbed by a surrounding PCM. In order to enhance heat transfer into the PCM, fins of width $2w$ and length $2L$ are provided periodically with a fin-to-fin pitch of $2\,W$, as shown in Fig. 1(a). Thermal conductivity of fin and PCM are k_f and k_p respectively. Similar nomenclature is followed for the volumetric specific heat c. The latent heat of phase change of the PCM is taken to be L_p. All properties are assumed to be independent of temperature. The PCM and fin are both assumed to be initially at the PCM melting temperature T_m. Note that if infinite time is available for heat transfer, then the entire PCM will eventually reach the wall temperature, so that the total heat absorbed is proportional to PCM mass, and therefore, the presence of the fin may actually reduce the amount of energy storage by reducing PCM available within the fixed total volume. However, in several applications, only a finite time is available for energy storage, in which case, transient heat transfer in the fin may enhance the total energy absorbed within the finite available time. Even accounting for the reduced PCM mass, this may result in overall increase in energy absorbed, compared to the case without fin.

The interest here is in determining the transient temperature distributions $T_f(x,t)$ and $T_p(x,y,t)$ in the fin and PCM respectively, and therefore, in determining the total amount of heat absorbed by the PCM, $q_{total}(t)$ for a given, finite total time. The fin provides additional surface for the PCM to absorb heat from. However, presence of the fin also reduces the area of direct contact between the PCM and the hot wall, which is the primary energy source in this problem. Accounting for these competing factors is, therefore, critical for accurate determination of $q_{total}(t)$.

The analysis of this problem can be simplified by considering a symmetry unit cell that repeats itself in the geometry, as marked in Fig. 1(a) and shown in detail in Fig. 1(b). The total heat absorbed by the PCM up to time t, $q_{total}(t)$, comprises two distinct components – $q_1(t)$, the heat absorbed by the PCM directly from the width $(W\text{-}w)$ of the wall, and $q_2(t)$, the heat absorbed by the PCM from the length L of the fin, as shown in Fig. 1(b). Thermal diffusion from the wall into the fin slowly raises the fin temperature, which in turn increases the heat absorbed by the PCM. Thus, $q_2(t)$ is expected to be small initially and slowly rise with time. In general, $q_2(t)$ will depend on the properties of both fin and PCM as well as geometrical parameters such as fin size w. On the other hand, $q_1(t)$ depends only on the properties of the PCM and the temperature difference $(T_w - T_m)$. The region close to the origin of the coordinate axis shown in Fig. 1(a) experiences heat absorption from both directions. Neglecting this small region, two separate, independent melting fronts can be assumed for ease of analysis in the rest of the PCM. The melting fronts originating from the wall and fin propagate in the x and y directions, respectively, and are responsible for $q_1(t)$ and $q_2(t)$, respectively. Such an assumption of two independent melting fronts is commonly made to simplify two-dimensional phase change problems [16–18], and is reasonable when the aspect ratio of the unit cell is much larger than one. Further, natural convection in the liquid phase is neglected here, which may be a reasonable assumption for a wide, horizontal PCM layer [7].

Separate expressions for $q_1(t)$ and $q_2(t)$ are now derived. For generality, the results are derived in non-dimensional form. The non-dimensionaliztion scheme is described in the Nomenclature section. Non-dimensional temperature is denoted as θ, whereas several other non-dimensional quantities are denoted with an overbar.

2.1. Wall-to-PCM heat transfer

Until the time that the phase change front originating from the wall reaches the other end of the domain, the PCM may be considered to be semi-infinite. Under this assumption, the problem of heat transfer from the wall directly into the PCM is the classical Stefan problem with T_w as the constant temperature boundary condition. Therefore, the location of the phase change front and temperature distribution in the melted PCM are given by [26]

$$\bar{x}_{LS}(\bar{t}) = 2\lambda\sqrt{\bar{t}} \tag{1}$$

$$\theta_P(\bar{x},\bar{t}) = 1 - \frac{\mathrm{erf}\left(\frac{\bar{x}}{2\sqrt{\bar{t}}}\right)}{\mathrm{erf}(\lambda)} \tag{2}$$

where λ is the root of:

$$\lambda \mathrm{erf}(\lambda) e^{\lambda^2} = \frac{Ste}{\sqrt{\pi}} \tag{3}$$

Consequently, the total heat absorbed by the PCM directly from the wall $\bar{q}_1(\bar{t})$ is given by

$$\bar{q}_1(\bar{t}) = 2\left(1 - \frac{w}{W}\right)\frac{\sqrt{\bar{t}}}{\sqrt{\pi}\,\mathrm{erf}(\lambda)} \tag{4}$$

Note that Eq. (4) accounts for the reduced area of contact between the PCM and the wall due to presence of the fin. Therefore, the larger the fin size *w/W*, the lower is the value of $\bar{q}_1(\bar{t})$.

2.2. Wall-to-fin-to-PCM heat transfer

The problem of determining $\bar{q}_2(\bar{t})$, the total heat absorbed by the PCM through the fin is considerably more complicated due to the coupling between thermal conduction into the fin and heat transfer from fin into the PCM. This necessitates determining the fin temperature distribution $\theta_f(\bar{x},\bar{t})$ first, followed by the PCM temperature distribution $\theta_p(\bar{x},\bar{y},\bar{t})$, and then $\bar{q}_2(\bar{t})$.

Temperature within the fin is assumed to vary spatially only in the *x* direction, and not in the *y* direction. This assumption of one-dimensional heat transfer in the fin is reasonable as long as the fin width is small compared to fin length. In order to determine the fin temperature distribution, the governing energy conservation equation in the fin is derived. To do so, energy balance of an infinitesimal fin element of length *dx* is considered, as shown in Fig. 2. Similar to the classical energy analysis of a fin in a fluid without phase change [27], the components of energy balance to be considered include thermal conduction into and out of the element, increase in thermal energy stored in the element and heat loss from the element into the PCM. As shown in Fig. 2, a balance between these terms, along with Fourier's law can be used to derive the following governing equation for the fin temperature

$$\frac{\bar{c}_f}{\bar{k}_f}\frac{\partial \theta_f}{\partial \bar{t}} = \frac{\partial^2 \theta_f}{\partial \bar{x}^2} - \bar{S} \tag{5}$$

where $\bar{S}$ is the heat generation term due to heat transfer to the PCM. The final step is to express $\bar{S}$ in the form of the fin temperature, in order to write Eq. (5) as a differential equation in θ_f. In traditional fin analysis in a fluid without phase change [27], this can be done simply using the convective heat transfer coefficient. In the present analysis, however, this term is much more challenging to write in terms of θ_f due to phase change occurring in the PCM. Temperature of the fin element changes over time, and therefore, this is a time-dependent boundary condition problem, unlike the wall-to-PCM problem which can be easily modeled as a classical Stefan problem with constant temperature boundary condition. In order to determine the PCM temperature distribution, and therefore heat flux into the PCM due

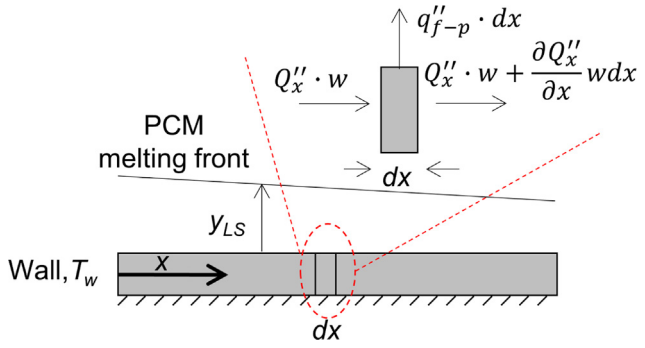

Fig. 2. Schematic of an infinitesimal fin element of width *dx* for deriving a governing energy conservation equation for the fin temperature distribution.

to the time-varying fin temperature that acts as the base temperature for this phase change problem, this must be treated as a one-dimensional melting problem with time-dependent temperature boundary condition given by the fin temperature. A solution for this problem using perturbation method is available [28,29]. In this method, the temperature distribution in the PCM is written in a power series form, using the Stefan number, and the independent variable is transformed from $\bar{t}$ to $\bar{y}$, the phase change front location. Finally, utilizing the energy conservation equation at the phase change interface, and carrying out a term-by-term comparison for various powers of *Ste*, an expression for the temperature distribution can be derived. The final result is [28,29]

$$\theta_p(\bar{x},\bar{y},\bar{t}) = \theta_0(\bar{x},\bar{y},\bar{t}) + Ste\,\theta_1(\bar{x},\bar{y},\bar{t}) + Ste^2\theta_2(\bar{x},\bar{y},\bar{t}) \tag{6}$$

where the components θ_0, θ_1 and θ_2 may be expressed in terms of the corresponding fin temperature at the location *x* as follows

$$\theta_0(\bar{x},\bar{y},\bar{t}) = \theta_f\left(1 - \frac{\bar{y}}{\bar{y}_{LS}}\right) \tag{7}$$

$$\theta_1(\bar{x},\bar{y},\bar{t}) = \frac{1}{6}\theta_f\left(\frac{\bar{y}}{\bar{y}_{LS}}\right)\left(\frac{\bar{y}}{\bar{y}_{LS}} - 1\right)\left[\theta_f\left(\frac{\bar{y}}{\bar{y}_{LS}} + 1\right) - \frac{\theta_f'}{\bar{y}_{LS}'}\bar{y}_{LS}\left(\frac{\bar{y}}{\bar{y}_{LS}} - 2\right)\right] \tag{8}$$

$$\theta_2(\bar{x},\bar{y},\bar{t}) = -\frac{1}{360}\theta_f\left(\frac{\bar{y}}{\bar{y}_{LS}}\right)\left(\frac{\bar{y}}{\bar{y}_{LS}} - 1\right)\left[\theta_f^2\left(\frac{\bar{y}}{\bar{y}_{LS}} + 1\right)\left(9\left(\frac{\bar{y}}{\bar{y}_{LS}}\right)^2 + 19\right) + 10\left(\frac{\theta_f'}{\bar{y}_{LS}'}\right)^2\bar{y}_{LS}^2\left(\frac{\bar{y}}{\bar{y}_{LS}} + 4\right) + 5\theta_f\frac{\theta_f'}{\bar{y}_{LS}'}\bar{y}_{LS}\left(3\left(\frac{\bar{y}}{\bar{y}_{LS}}\right)^2 + 5\left(\frac{\bar{y}}{\bar{y}_{LS}}\right) + 17\right)\right] \tag{9}$$

where θ_f is the fin temperature distribution. As a result, an expression for $\bar{S}$ can be written as

$$\bar{S} = \frac{1}{\bar{k}_f\frac{w}{W}}\left[\frac{\theta_f}{\bar{y}_{LS}} + Ste\frac{\theta_f\left(\theta_f + 2\frac{\theta_f'}{\bar{y}_{LS}'}\bar{y}_{LS}\right)}{6\bar{y}_{LS}} - Ste^2\frac{\theta_f\left(40\left(\frac{\theta_f'}{\bar{y}_{LS}'}\right)^2\bar{y}_{LS}^2 + 85\theta_f\frac{\theta_f'}{\bar{y}_{LS}'}\bar{y}_{LS} + 19\theta_f^2\right)}{360\bar{y}_{LS}}\right] \tag{10}$$

where the location of the melting front originating from the fin, $\bar{y}_{LS}$ is given by [28,29]

$$\bar{y}_{LS}(\bar{x},\bar{t}) = \left[2Ste\int_0^{\bar{t}}\theta_f(\bar{x},\bar{\tau})\left(1 - \frac{Ste}{3}\theta_f(\bar{x},\bar{\tau}) + \frac{7}{45}Ste^2\theta_f(\bar{x},\bar{\tau})^2\right)d\bar{\tau}\right]^{\frac{1}{2}} \tag{11}$$

Note that the primes in Eqs. (8)–(10) refer to time derivatives.

The perturbation method solution utilized above is valid only for small values of *Ste*, which is usually the case for most practical phase change processes [28,29], and only until the phase change front reaches the other boundary.

Eqs. (10) and (11) express heat loss from a fin location at any given time in terms of the prior fin temperature history at that location and thermal properties of the PCM.

By combining Eqs. (5) and (10), a complicated partial differential equation for the fin temperature distribution can be written as

$$\frac{\bar{c}_f}{\bar{k}_f}\frac{\partial \theta_f}{\partial \bar{t}} = \frac{\partial^2 \theta_f}{\partial \bar{x}^2} - \frac{1}{\bar{k}_f\frac{w}{W}}\left[\frac{\theta_f}{\bar{y}_{LS}} + Ste\frac{\theta_f\left(\theta_f + 2\frac{\theta_f'}{\bar{y}_{LS}'}\bar{y}_{LS}\right)}{6\bar{y}_{LS}} - Ste^2\frac{\theta_f\left(40\left(\frac{\theta_f'}{\bar{y}_{LS}'}\right)^2\bar{y}_{LS}^2 + 85\theta_f\frac{\theta_f'}{\bar{y}_{LS}'}\bar{y}_{LS} + 19\theta_f^2\right)}{360\bar{y}_{LS}}\right] \tag{12}$$

Note that the negative heat generation term in Eq. (12) involves the phase change front $\bar{y}_{LS}$, which itself is given by an integral of the fin temperature distribution over time (Eq. (11)). This makes Eq. (12) considerably complicated to solve explicitly.

Boundary conditions and initial conditions must be specified in order to complete the fin temperature problem. While at $\bar{x} = 0$, the fin temperature must equal the wall temperature, an adiabatic boundary condition applies at $\bar{x} = \bar{L}$ as a result of symmetry in the problem. Finally, the initial fin temperature is equal to the PCM melting temperature. These are given mathematically by the following:

$$\theta_f(0,\bar{t}) = 1 \tag{13}$$

$$\left(\frac{\partial\theta_f}{\partial\bar{x}}\right)_{\bar{x}=\bar{L}} = 0 \tag{14}$$

$$\theta_f(\bar{x},0) = 0 \tag{15}$$

Eq. (12) captures the effect of the PCM in the form of a negative heat generation term, similar to classical fin analysis without phase change [27]. This term involves an integral of the temperature distribution over time, which, although more complicated than past work [16–18], is more accurate, as it correctly accounts for propagation of the phase change front over time.

Once a solution for Eq. (12) is determined, the PCM temperature distribution can be obtained from Eq. (6). Heat transfer in the x direction within the PCM is neglected, which is reasonable in the absence of flow within the PCM. Finally, an expression for $\bar{q}_2(\bar{t})$, the total heat flux into the PCM at the fin base up to time $\bar{t}$ can be derived using Eq. (10) as

$$\bar{q}_2(\bar{t}) = \int_0^{\bar{t}}\int_0^{\bar{L}} \left[\frac{\theta_f}{\bar{y}_{LS}} + Ste\frac{\theta_f\left(\theta_f + 2\frac{\theta_f'}{\bar{y}_{LS}}\bar{y}_{LS}\right)}{6\bar{y}_{LS}} - (Ste)^2\frac{\theta_f\left(40\left(\frac{\theta_f'}{\bar{y}_{LS}}\right)^2\bar{y}_{LS}^2 + 85\theta_f\frac{\theta_f'}{\bar{y}_{LS}}\bar{y}_{LS} + 19\theta_f^2\right)}{360\bar{y}_{LS}} \right] d\bar{x}d\bar{t} \tag{16}$$

This approach for calculating the total heat absorbed by the PCM from the fin requires a solution for the fin temperature distribution governed by Eqs. (12)–(15). Eq. (12) is a generalization of a previously presented treatment [16] in which sensible heat storage was neglected and the phase change front was assumed to be constant in the fin equation. In contrast, Eq. (12) correctly accounts for transient changes in the phase change front, as well as the effect of transient changes in the fin temperature on the phase change front.

While a completely analytical solution for Eq. (12) is quite unlikely due to its considerable complexity, this equation provides an explicit expression for the derivative of fin temperature with time. As a result, a numerical time-stepping method may be appropriate for solving Eq. (12). An implicit approach is used to ensure stability of the computations. The fin length is divided into 401 nodes. A non-dimensional timestep of 3.34×10^{-5} is used after ensuring that further shorter time steps did not significantly change the results. At each time step, a set of coupled linear algebraic equations in the unknown temperatures at the nodes are set up and solved using matrix inversion. The resulting temperature distribution is used to repeat this process at the next timestep and therefore march forward in time.

One practical challenge is that at $\bar{t} = 0$, θ_f and $\bar{y}_{LS}$ are both zero, and therefore, the negative heat generation term in Eq. (12) cannot be computed. This singularity makes it difficult to initiate the time-stepping process. In order to overcome this difficulty, an approximation is made for an initial time period $0<\bar{t}<\bar{t}^*$, during which, heat transfer from the fin into the PCM is neglected in Eq. (12). As a result, during this period, temperature distribution in the fin is approximated to be governed only by diffusion from the hot wall. Under this approximation, the temperature distribution during this period can be easily derived using the method of separation of variables [26] as

$$\theta_f(\bar{x},\bar{t}) = 1 - 2\sum_{n=1}^{\infty}\frac{(1-\cos(\beta_n))}{\beta_n}\sin(\beta_n\bar{x})e^{-\beta_n^2\bar{t}} \tag{17}$$

where

$$\beta_n = (2n-1)\frac{\pi}{2} \tag{18}$$

for $n = 1,2,3\ldots$

Eq. (17), along with the phase change front location at $\bar{t} = \bar{t}^*$ calculated using the fin temperature can be used in Eq. (12) in order to calculate $\frac{\partial\theta_f}{\partial\bar{t}}$ at $\bar{t}=\bar{t}^*$, and therefore, carry out time-stepping for the fin temperature distribution starting at $\bar{t} = \bar{t}^*$. In order to minimize the error introduced by ignoring heat transfer from fin to PCM up to $\bar{t} = \bar{t}^*$in this approach, the value of $\bar{t}^*$ must be chosen to be small compared to the total time period. The effect of $\bar{t}^*$ on the accuracy of the solution is examined later.

Considering both components of heat absorbed, an expression for the total heat absorbed by the PCM in a certain time t can be written as

$$\bar{q}_{total}(\bar{t}) = \bar{q}_1(\bar{t}) + \bar{q}_2(\bar{t}) = 2\left(1-\frac{w}{W}\right)\frac{\sqrt{\bar{t}}}{\sqrt{\pi}\,\mathrm{erf}(\lambda)} + \int_0^{\bar{t}}\int_0^{\bar{L}} \left[\frac{\theta_f}{\bar{y}_{LS}} + Ste\frac{\theta_f\left(\theta_f + 2\frac{\theta_f'}{\bar{y}_{LS}}\bar{y}_{LS}\right)}{6\bar{y}_{LS}} - (Ste)^2\frac{\theta_f\left(40\left(\frac{\theta_f'}{\bar{y}_{LS}}\right)^2\bar{y}_{LS}^2 + 85\theta_f\frac{\theta_f'}{\bar{y}_{LS}}\bar{y}_{LS} + 19\theta_f^2\right)}{360\bar{y}_{LS}} \right] d\bar{x}d\bar{t} \tag{19}$$

Eq. (19) shows that $\bar{q}_{total}$ has a non-monotonic dependence on w/W. As the value of w/W increases, $\bar{q}_2(\bar{t})$, heat absorbed from the fin increases due to better thermal conduction into the fin, leading to higher fin temperature and therefore greater heat transfer into the PCM. However, as the value of w/W increases, the heat absorbed directly from the wall, $\bar{q}_1(\bar{t})$, decreases. While the relationship between w/W and $\bar{q}_1(\bar{t})$ is quite explicit, as shown in Eq. (4), the dependence of $\bar{q}_2(\bar{t})$ on w/W is more complicated because the solution for the differential equation for $\theta_f(\bar{x},\bar{t})$, and hence the PCM temperature distribution is not straightforward.

2.3. Alternate derivation of fin temperature equation

The expression for the source term in Eq. (10) is derived by applying Fourier's law at the fin-PCM interface on the PCM temperature distribution given by the perturbation method solution. An alternate expression for the source term can be written by adding up latent and sensible heat storage rates in the PCM as follows:

$$\bar{S} = \frac{1}{\bar{k}_f\frac{w}{W}}\left[\frac{1}{Ste}\frac{\partial\bar{y}_{LS}}{\partial\bar{t}} + \int_0^{\bar{y}_{LS}}\frac{\partial\theta_f}{\partial\bar{t}}d\bar{y}\right] \tag{20}$$

Note that a similar analysis of this problem in the past [16] had neglected the sensible component for heat transfer from fin into the PCM.

By combining Eqs. (20) and (5), an alternate form of the governing equation for the fin temperature distribution can be derived to be

$$\frac{\bar{c}_f}{\bar{k}_f}\frac{\partial\theta_f}{\partial\bar{t}} = \frac{\partial^2\theta_f}{\partial\bar{x}^2} - \frac{1}{\bar{k}_f\frac{w}{W}}\left[\frac{1}{Ste}\frac{\partial\bar{y}_{LS}}{\partial\bar{t}} + \int_0^{\bar{y}_{LS}}\frac{\partial\theta_f}{\partial\bar{t}}d\bar{y}\right] \tag{21}$$

Eqs. (21) and (12) are expected to result in the same fin temperature distribution since the heat loss into the PCM can be equivalently computed by either applying Fourier's law at the fin-PCM interface, or by adding up sensible and latent heat storage in the PCM. Eq. (21) is more complicated than Eq. (12) to solve, due to which, Eq. (12) is used in this work for understanding and optimizing heat transfer into the PCM in presence of a fin.

3. Results and discussion

3.1. Model validation

Validation of the analytical model presented in Section 2 is carried out by comparison with finite-element simulations. For this purpose, octadecane paraffin wax PCM with an aluminum fin, similar to Fig. 1(b) is considered. Thermal conductivity, heat capacity, density and latent heat of the PCM are taken to be 0.15 W/m K, 2300 J/kg K, 780 kg/m^3 and 244000 J/kg, respectively, corresponding to the properties of octadecane [30]. Standard values are used for thermal properties of the aluminum fin. Temperature fields in the fin and PCM are computed using the enthalpy method and the finite element technique. Grid independence is ensured by verifying minimal change in predicted temperature beyond 399,600 nodes in the PCM and 44,400 nodes in the fin. The PCM is defined as a homogenous binary mixture of solid and liquid phases that is initially all solid. Wall temperature is taken to be 20 K higher than the PCM melting point. The phase change process is simulated using the enthalpy method [26] which defines the phase change material as a binary mixture of liquid and solid. Thermal properties of each phase and a reference enthalpy of fusion are defined.

Fig. 3(a) shows a comparison of fin temperature distribution determined from the analytical model presented in Section 2 with finite-element simulation results at multiple times. The analytical model is found to be in good agreement with finite-element simulations at each of the plotted times. Fig. 3(b) plots the location of the phase change front along the fin at multiple times. Similar to Fig. 3(a), good agreement is obtained between the analytical model and finite-element simulations. Note that these calculations use a value of $\bar{t}^* = 3.34 \times 10^{-5}$, which represents only 0.05% of the total time. The small value of $\bar{t}^*$ minimizes the error associated with the approximation needed at early time.

Further, Fig. 4 presents colormaps of temperature distribution in the PCM and fin at multiple times predicted by the finite-element simulations. Heat diffusion into the fin, as well as heat transfer into the PCM through two distinct mechanisms – direct conduction from wall on the left, and conduction through the fin on the bottom – are all clearly seen in these plots. Two nearly-independent phase change fronts originating from the PCM-wall and PCM-fin interfaces are seen. These plots show that at each time, the melting fronts from the left and bottom do not interact significantly with each other, except for a small region close to $\bar{x} = 0$ is det. This justifies a key assumption in the analytical model presented in Section 2.

3.2. Optimal value of w/W

Fig. 5(a)–(f) plot the two components of heat transfer into the PCM as well as total heat transferred up to $\bar{t} = 6.69 \times 10^{-2}$ determined from Eqs. (4), (16) and (19) as functions of the relative fin size *w/W* for multiple values of fin thermal conductivity $\bar{k}_f$. Other thermophysical properties are held constant. For comparison, the total non-dimensional heat absorbed in a baseline case with no fin is 0.895.

These plots clearly show that the larger the fin thermal conductivity, the higher is the heat absorbed. However, for a fixed fin thermal conductivity, each of these Figures show the existence of an optimal value of *w/W* that maximizes total heat absorbed. As *w/W* increases, the reduced thermal resistance of the fin results in greater heat transfer into the fin, higher fin temperature and therefore, $\bar{q}_2$ increases with *w/W*. However, an increase in *w/W* is also seen to result in a reduction in $\bar{q}_1$, because a larger value of *w/W* results in a greater area of the wall being occupied by the fin, and therefore reduces the area of contact directly between the wall and the PCM. While $\bar{q}_1$ reduces linearly with *w/W*, the increase in $\bar{q}_2$ with *w/W* is sharp initially, and then linear. The total heat absorbed from the wall and fin, given by the sum of $\bar{q}_1$ and $\bar{q}_2$, plotted in Fig. 5(a)–(f) has a non-monotonic dependence on *w/W*. with a peak occurring at a reasonably low value of *w/W*. This means that even a very small fin width provides sufficient thermal conductance into the fin to positively impact the total heat flow into the PCM. Beyond this peak value, further increasing the fin size is not beneficial because at the peak, thermal resistance of the fin is already quite low and does not reduce meaningfully by increasing *w/W* further. When this state is reached, further increase in *w/W* reduces $\bar{q}_1$ without contributing much towards increasing $\bar{q}_2$. This is further illustrated in Fig. 6 which plots fin temperature distribution at $\bar{t} = 6.69 \times 10^{-2}$ for different values of *w/W*, with $\bar{k}_f$ = 1333. Fig. 6 shows sharp increase in fin temperature distribution with increasing *w/W* when *w/W* is small. However, this effect saturates when *w/W* is somewhat large because at that point, further increasing *w/W* does not significantly reduce thermal resistance of the fin, which is already quite low. This illustrates the impor-

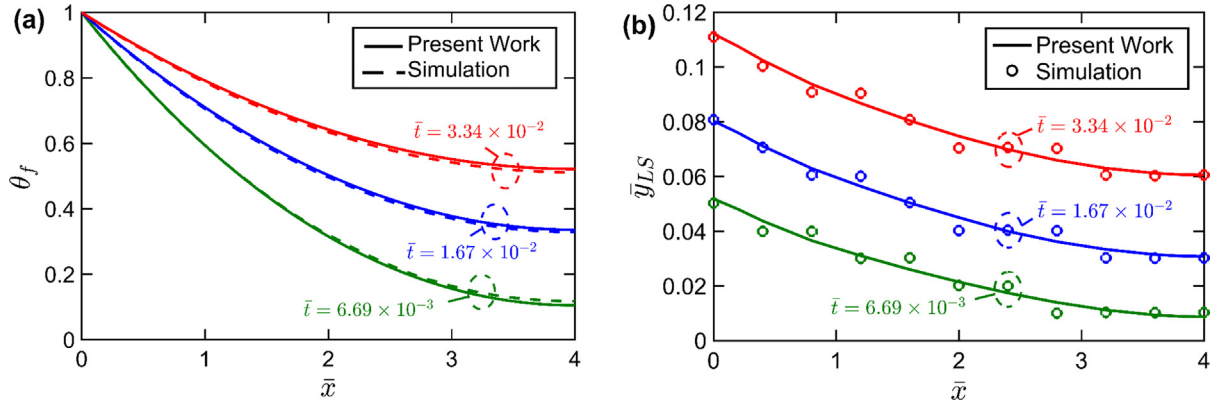

Fig. 3. Validation of results by comparison between theoretical model and finite-element simulations. (a) Temperature distribution in the fin at multiple times; (b) location of the phase change front across the fin at multiple times. In these plots, $\frac{w}{W} = 0.1$, $\bar{L} = 4$, *Ste* = 0.19, $\bar{k}_f = 1580$ and $\bar{c}_f = 1.36$. Properties of octadecane and Aluminum are assumed for PCM and fin respectively.

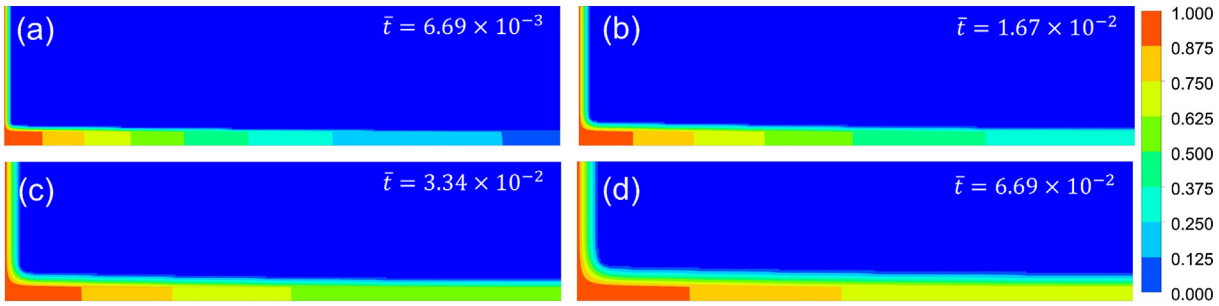

Fig. 4. Temperature map determined from finite-element simulations for the problem considered in Fig. 3. Location of the fin is emphasized with dark lines.

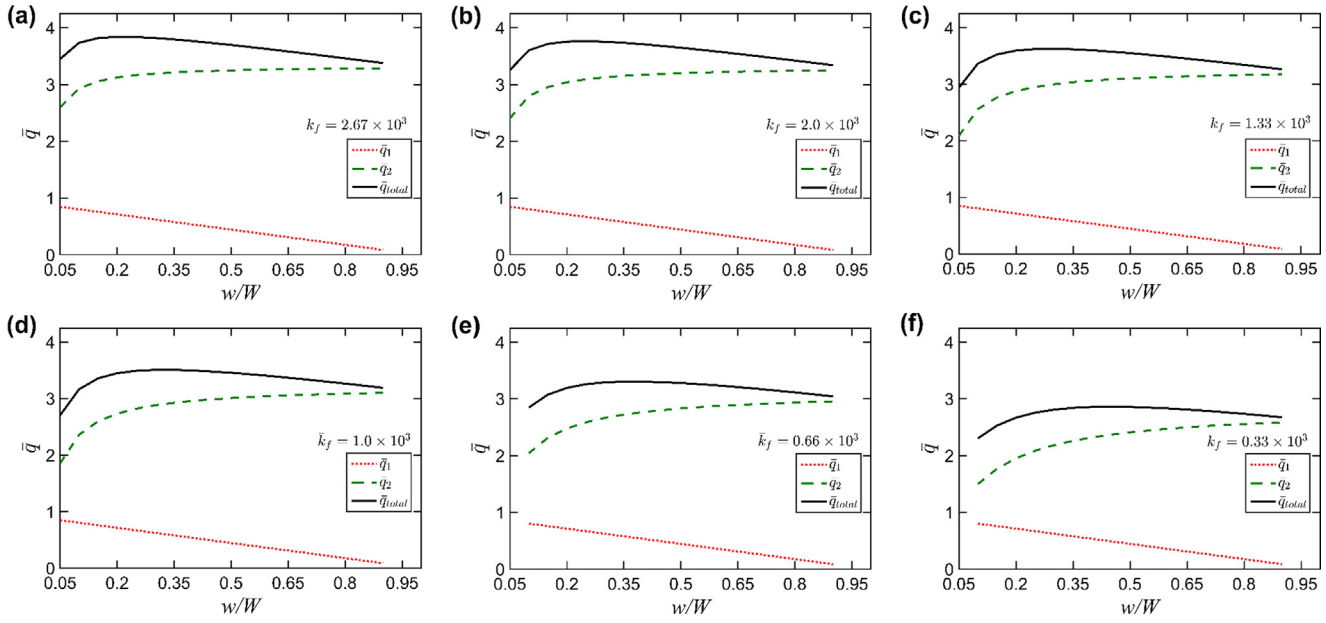

Fig. 5. Total heat absorbed by the PCM up to $\bar{t} = 6.69 \times 10^{-2}$, including the wall and fin components. (a)–(f) present plots for six different fin thermal conductivities. In these plots, $\bar{L} = 4$, $Ste = 0.19$ and $\bar{c}_f = 1.36$.

tance of carefully choosing the fin size relative to the wall in order to balance the two conflicting considerations in maximizing overall heat transfer into the PCM.

Thermal conductivity of the fin plays a key role in determining the optimal value of *w/W*. Fig. 7(a) plots the total heat absorbed as a function of *w/W* for multiple values of $\bar{k}_f$. These curves clearly show a distinct shift in the location of the maxima as $\bar{k}_f$ reduces. Fig. 7(b) plots the optimal value of *w/W* corresponding to the peak as a function of $\bar{k}_f$. This plot shows that the higher the value of $\bar{k}_f$, the lower is the value of *w/W* at which the peak of stored energy occurs. This is because thermal resistance of a high thermal conductivity fin saturates at a lower fin size, whereas thermal resistance of a low thermal conductivity fin can continue to improve as the fin size increases. The dependence of peak energy storage performance on thermal conductivity illustrated in Fig. 7(a) and (b) is important to account for in practical fin design because if the fin size is greater than the optimal value for the thermal conductivity of the fin, then the fin is counter-productive and actually impedes flow of heat into the PCM.

3.3. Effect of time available for heat transfer

The total time available for heat transfer into the PCM plays a key role in determining the impact of the fin. In principle, if infinite time is available, then the PCM will eventually reach the wall temperature, and therefore, the presence of the fin is un-necessary and counter-productive, since it reduces PCM volume. However, when only a short time is available, the fin may contribute towards increasing overall energy storage by offering an alternate path for heat transfer into the PCM. The dependence of the optimal fin size on available time is investigated. Fig. 8 plots the optimal value of *w/W* that results in the highest possible total energy stored as a function of the total time available for heat transfer. Fig. 8 shows that as time increases, the optimal fin becomes thinner and thinner. This happens because at larger times, the role of the fin in increasing surface area and promoting indirect heat transfer into the PCM diminishes, and the negative impact of reduced PCM volume and reduced area of wall-PCM contact becomes more and more important. Fig. 8 illustrates the important role of available time on the optimal design of the fin for promoting heat transfer into the PCM.

3.4. Impact of thermal properties

Fig. 9 examines the effect of material thermal properties on energy storage performance. Total heat absorbed by the PCM with $w/W = 0.2$ up to $\bar{t} = 6.69 \times 10^{-2}$ is plotted as a function of $\bar{k}_f$ in Fig. 9 for octadecane PCM. The two components of total heat absorbed – $\bar{q}_1$ and $\bar{q}_2$ – are also plotted for comparison. Fig. 9 shows that while $\bar{q}_1$ remains unchanged with increasing $\bar{k}_f$ because fin

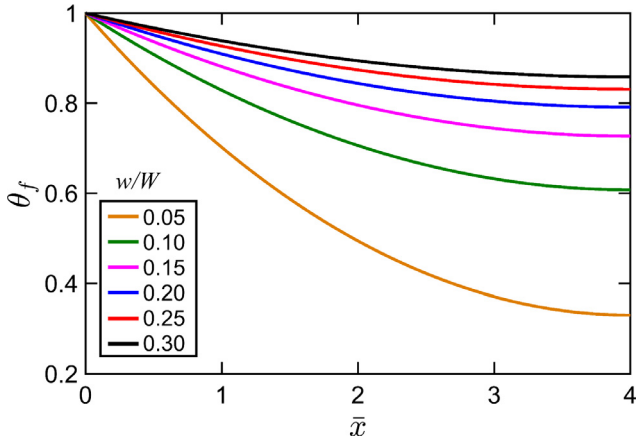

Fig. 6. Fin temperature distribution at $\bar{t} = 6.69 \times 10^{-2}$ for multiple values of *w/W*, showing the saturation impact of *w/W*. In this plot, $\bar{k}_f = 1333$, *Ste* = 0.19, $\bar{c}_f = 1.36$, $\bar{L} = 4$.

thermal conductivity does not affect heat absorbed directly from the wall, $\bar{q}_2$ increases with $\bar{k}_f$ because of the increased thermal diffusion into the fin and therefore enhanced heat transfer into the PCM. On the overall, the total energy absorbed by the PCM increases with increasing k_f.

3.5. Impact of sensible heat storage

Fig. 10 examines the importance of accounting for latent and sensible heat storage in the PCM on the results of the analytical model. In the alternate derivation of the fin temperature equation, the heat loss term, Eq. (20), has explicit terms for the contributions of latent and sensible heat storage mechanisms. Using the resulting Eq. (21) for determining the fin temperature distribution, Fig. 10 plots fin temperature distribution at multiple times without and with sensible heat storage accounted for. Plots are presented in Fig. 10(a) and (b) for two different values of the wall temperature relative to the melting temperature. For a relatively small value of *Ste* = 0.19, the error involved in neglecting sensible heat storage is found to be reasonably small. However, for a larger value of *Ste* = 0.94, the error is much more significant. Fig. 10 shows that this error also grows as time increases.

3.6. Effect of $\bar{t}^*$

Determining the fin temperature distribution from Eq. (12) requires an approximation to handle the singularity at $\bar{t} = 0$, wherein heat transfer into the fin is assumed to occur without heat loss to the PCM for a short initial time, up to $\bar{t} = \bar{t}^*$. Clearly, the larger the value of $\bar{t}^*$, the greater is the error incurred due to neglecting the heat loss into PCM. Fig. 11 plots temperature distribution in

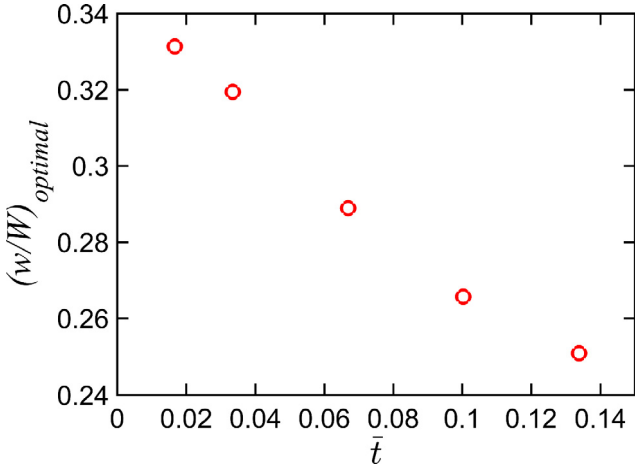

Fig. 8. Effect of total time available for heat transfer on the optimal fin thickness that maximizes total amount of heat stored. In this plot, *Ste* = 0.19, $\bar{c}_f = 1.36$, $\bar{L} = 4$ and $\bar{k}_f = 1333$.

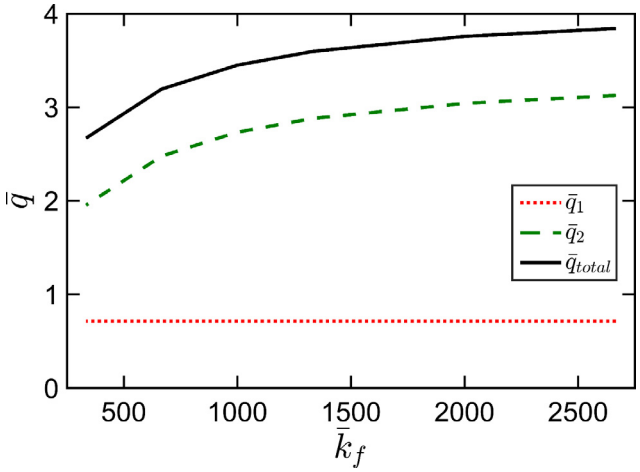

Fig. 9. Effect of fin thermal conductivity on heat absorbed from the wall and fin, as well as total heat absorbed up to $\bar{t} = 6.69 \times 10^{-2}$. In this plot, *w/W* = 0.2, *Ste* = 0.19, $\bar{c}_f = 1.36$, $\bar{L} = 4$.

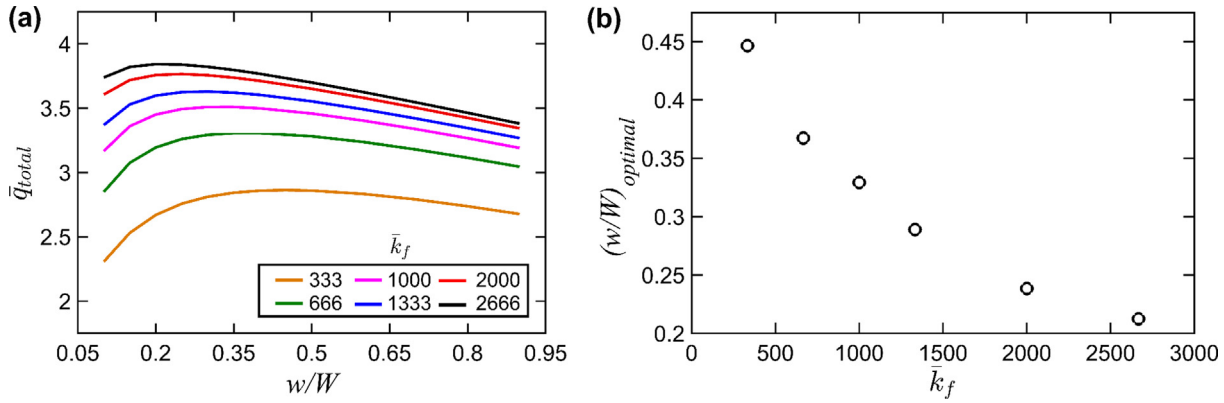

Fig. 7. (a) Plot of $\bar{q}_{total}$ at $\bar{t} = 6.69 \times 10^{-2}$ as a function of *w/W* for different values of fin thermal conductivity. (b) Optimal value of *w/W* as a function of fin thermal conductivity. In these plots, *Ste* = 0.19, $\bar{c}_f = 1.36$, $\bar{L} = 4$.

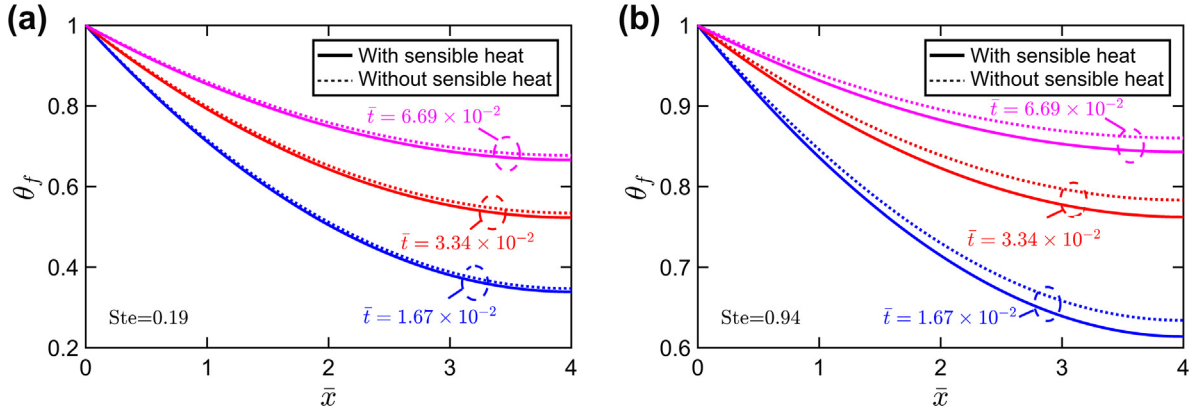

Fig. 10. Effect of accounting for sensible heat storage. (a) and (b) plot fin temperature distribution at different times for two different values of *Ste*. In these plots, $w/W = 0.1$, $\bar{k}_f = 1580$, $\bar{c}_f = 1.36$ and $\bar{L} = 4$.

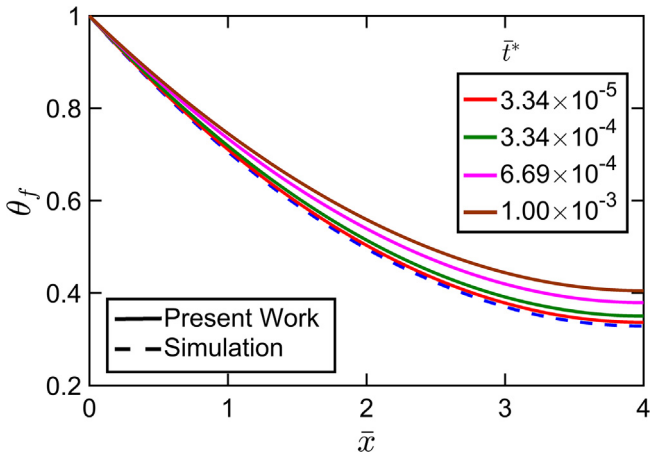

Fig. 11. Effect of the value of $\bar{t}^*$ on the accuracy of fin temperature distribution computed from equation (12) for a total time of $\bar{t} = 1.67 \times 10^{-2}$. Result from a finite-element simulation is also shown for comparison. In this plot, $w/W = 0.1$, $\bar{k}_f = 1580$, $\bar{c}_f = 1.36$ and $\bar{L} = 4$.

the fin at the final time $\bar{t} = 1.67 \times 10^{-2}$ for multiple values of $\bar{t}^*$. For comparison, a plot based on a finite-element simulation that does not incur this error is also presented. Fig. 11 clearly shows significant error when $\bar{t}^*$ is large. This error reduces rapidly as $\bar{t}^*$ reduces. In this specific case, a value of $\bar{t}^* = 3.34 \times 10^{-5}$, corresponding to 0.05% of the total time results in reasonable agreement between the analytical model and finite-element simulation. Note that the need to utilize an initial period that neglects heat loss into the PCM results from the singularity in Eq. (12) that makes it impossible to initiate time-stepping at $\bar{t}$=0 to compute the fin temperature distribution as a function of time.

4. Conclusions

It is important to complement experimental research on enhancement of phase change energy storage through extended surfaces with theoretical modeling of heat transfer in such systems. The transient and non-linear nature of heat transfer in such processes results in complicated governing equations for the temperature distribution. The equations derived in this work correctly account for several phenomena that were unaccounted for in past papers, including sensible heat storage in the newly formed phase and transient variation in phase change front location. Consequently, this work establishes the existence of an optimal fin size that maximizes the benefit of the fin on heat transfer into the PCM.

From a theoretical perspective, this work generalizes the well-known, linear differential equation for steady-state temperature distribution for a fin in a single phase fluid to a significantly more complicated non-linear differential equation for a fin in a phase change material. From a practical perspective, the fin temperature distribution and the consequent computation of heat absorbed by the PCM are critical insights, and offer guidelines for the optimal design of phase change energy storage systems that occur in several engineering applications. Specifically, the optimal fin size for maximum heat transfer into the PCM, and the dependence of this optimal fin size on thermal properties and the available time window are both important and practical guidelines.

The present work neglects the effect of natural convection in the liquid phase, which, while not important for the geometry considered here, may be significant in other scenarios, for example, in a long, vertical PCM layer [7]. The effect of temperature-dependence of thermal properties, while neglected here, may also be important to account for in scenarios with relatively large temperature change.

Declaration of Competing Interest

None declared.

Acknowledgements

This material is based upon work supported by CAREER Award No. CBET-1554183 from the National Science Foundation.

References

[1] H. Zhang, J. Baeyens, J. Degrève, G. Cacères, Concentrated solar power plants: Review and design methodology, Renew. Sustain. Energy Rev. 22 (2013) 466–481, https://doi.org/10.1016/j.rser.2013.01.032.
[2] K. Bhagat, S.K. Saha, Numerical analysis of latent heat thermal energy storage using encapsulated phase change material for solar thermal power plant, Renewable Energy 95 (2016) 323–336, https://doi.org/10.1016/j.renene.2016.04.018.
[3] M. Kenisarin, K. Mahkamov, Solar energy storage using phase change materials, Renew. Sustain. Energy Rev. 11 (2007) 1913–1965, https://doi.org/10.1016/j.rser.2006.05.005.
[4] A. Sharma, V. Tyagi, C. Chen, D. Buddhi, Review on thermal energy storage with phase change materials and applications, Renew. Sustain. Energy Rev. 13 (2009) 318–345, https://doi.org/10.1016/j.rser.2007.10.005.
[5] J. Eftekhar, A. Haji-Sheikh, D.Y.S. Lou, Heat transfer enhancement in a paraffin wax thermal storage system, J. Sol. Energy Eng. 106 (1984) 299, https://doi.org/10.1115/1.3267599.
[6] W.R. Humphries, E.I. Griggs, A design handbook for phase change thermal control and energy storage devices, National Aeronautics and Space

Administration, Scientific and Technical Information Office, Washington, 1977. NASA Technical Paper 1074.
[7] V. Shatikian, G. Ziskind, R. Letan, Numerical investigation of a PCM-based heat sink with internal fins, Int. J. Heat Mass Transf. 48 (2005) 3689–3706, https://doi.org/10.1016/j.ijheatmasstransfer.2004.10.042.
[8] T. Rozenfeld, Y. Kozak, R. Hayat, G. Ziskind, Close-contact melting in a horizontal cylindrical enclosure with longitudinal plate fins: Demonstration, modeling and application to thermal storage, Int. J. Heat Mass Transf. 86 (2015) 465–477, https://doi.org/10.1016/j.ijheatmasstransfer.2015.02.064.
[9] Y. Kozak, T. Rozenfeld, G. Ziskind, Close-contact melting in vertical annular enclosures with a non-isothermal base: Theoretical modeling and application to thermal storage, Int. J. Heat Mass Transf. 72 (2014) 114–127, https://doi.org/10.1016/j.ijheatmasstransfer.2013.12.058.
[10] H. Shmueli, G. Ziskind, R. Letan, Melting in a vertical cylindrical tube: Numerical investigation and comparison with experiments, Int. J. Heat Mass Transf. 53 (2010) 4082–4091, https://doi.org/10.1016/j.ijheatmasstransfer.2010.05.028.
[11] L.-W. Fan, Y.-Q. Xiao, Y. Zeng, X. Fang, X. Wang, X. Xu, et al., Effects of melting temperature and the presence of internal fins on the performance of a phase change material (PCM)-based heat sink, Int. J. Therm. Sci. 70 (2013) 114–126, https://doi.org/10.1016/j.ijthermalsci.2013.03.015.
[12] B. Kamkari, H. Shokouhmand, Experimental investigation of phase change material melting in rectangular enclosures with horizontal partial fins, Int. J. Heat Mass Transf. 78 (2014) 839–851, https://doi.org/10.1016/j.ijheatmasstransfer.2014.07.056.
[13] U. Stritih, An experimental study of enhanced heat transfer in rectangular PCM thermal storage, Int. J. Heat Mass Transf. 47 (2004) 2841–2847, https://doi.org/10.1016/j.ijheatmasstransfer.2004.02.001.
[14] A. Abhat, S. Aboul-Enein, N.A. Malatidis, Heat-of-fusion storage systems for solar heating applications, Therm. Storage Sol. Energy (1981) 157–171, https://doi.org/10.1007/978-94-009-8302-1_17.
[15] M. Huang, P. Eames, B. Norton, Thermal regulation of building-integrated photovoltaics using phase change materials, Int. J. Heat Mass Transf. 47 (2004) 2715–2733, https://doi.org/10.1016/j.ijheatmasstransfer.2003.11.015.
[16] P. Lamberg, K. Sirén, Approximate analytical model for solidification in a finite PCM storage with internal fins, Appl. Math. Model. 27 (2003) 491–513, https://doi.org/10.1016/s0307-904x(03)00080-5.
[17] P. Lamberg, Approximate analytical model for two-phase solidification problem in a finned phase-change material storage, Appl. Energy 77 (2004) 131–152, https://doi.org/10.1016/s0306-2619(03)00106-5.
[18] P. Lamberg, K. Sirén, Analytical model for melting in a semi-infinite PCM storage with an internal fin, Heat Mass Transf. 39 (2003) 167–176, https://doi.org/10.1007/s00231-002-0291-1.
[19] F. Talati, A.H. Mosaffa, M.A. Rosen, Analytical approximation for solidification processes in PCM storage with internal fins: imposed heat flux, Heat Mass Transf. 47 (2010) 369–376, https://doi.org/10.1007/s00231-010-0729-9.
[20] J. Leland, G. Recktenwald, Optimization of a phase change heat sink for extreme environments, in: Ninteenth Annual IEEE Semiconductor Thermal Measurement and Management Symposium, 2003. (n.d.). doi:10.1109/stherm.2003.1194384.
[21] R. Akhilesh, A. Narasimhan, C. Balaji, Method to improve geometry for heat transfer enhancement in PCM composite heat sinks, Int. J. Heat Mass Transf. 48 (2005) 2759–2770, https://doi.org/10.1016/j.ijheatmasstransfer.2005.01.032.
[22] P.P. Levin, A. Shitzer, G. Hetsroni, Numerical optimization of a PCM-based heat sink with internal fins, Int. J. Heat Mass Transf. 61 (2013) 638–645, https://doi.org/10.1016/j.ijheatmasstransfer.2013.01.056.
[23] A. Nagose, A. Somani, A. Shrot, A. Narasimhan, Genetic algorithm based optimization of PCM based heat sinks and effect of heat sink parameters on operational time, J. Heat Transfer 130 (2008), 011401.
[24] P.H. Biwole, D. Groulx, F. Souayfane, T. Chiu, Influence of fin size and distribution on solid-liquid phase change in a rectangular enclosure, Int. J. Therm. Sci. 124 (2018) 433–446, https://doi.org/10.1115/1.2780182.
[25] T. Bauer, Approximate analytical solutions for the solidification of PCMs in fin geometries using effective thermophysical properties, Int. J. Heat Mass Transf. 54 (2011) 4923–4930, https://doi.org/10.1016/j.ijheatmasstransfer.2011.07.004.
[26] D.W. Hahn, M.N. Özişik, Heat Conduction, third ed., John Wiley & Sons, Hoboken, New Jersey, 2012.
[27] T.L. Bergman, D.P. Dewit, A.S. Lavine, F.P. Incropera, Fundamentals of Heat and Mass Transfer, John Wiley & Sons, New Jersey, 2011.
[28] J. Caldwell, Y. Kwan, On the perturbation method for the Stefan problem with time-dependent boundary conditions, Int. J. Heat Mass Transf. 46 (2003) 1497–1501, https://doi.org/10.1016/s0017-9310(02)00415-5.
[29] G. Lock, J. Gunderson, D. Quon, J. Donnelly, A study of one-dimensional ice formation with particular reference to periodic growth and decay, Int. J. Heat Mass Transf. 12 (1969) 1343–1352, https://doi.org/10.1016/0017-9310(69)90021-0.
[30] N.R. Jankowski, F.P. McCluskey, A review of phase change materials for vehicle component thermal buffering, Appl. Energy 113 (2014) 1525–1561, https://doi.org/10.1016/j.apenergy.2013.08.026.